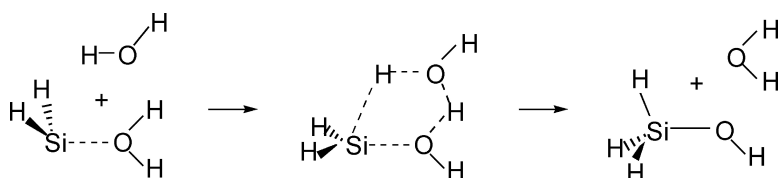Article

Experimental and Theoretical Evidence for Homogeneous Catalysis in the Gas-Phase Reaction of SiH with HO (and DO): A Combined Kinetic and Quantum Chemical Study

Rosa Becerra, Nicola Goldberg, J. Pat Cannady, Matthew J. Almond, J. Steven Ogden, and Robin Walsh

More About This Article

Additional resources and features associated with this article are available within the HTML version:

- Supporting Information
- Access to high resolution figures
- Links to articles and content related to this article
- Copyright permission to reproduce figures and/or text from this article

View the Full Text HTML

Experimental and Theoretical Evidence for Homogeneous Catalysis in the Gas-Phase Reaction of SiH₂ with H₂O (and D₂O): A Combined Kinetic and Quantum Chemical Study

Rosa Becerra,[†] Nicola Goldberg,[‡] J. Pat Cannady,[§] Matthew J. Almond,[‡]
J. Steven Ogden,[∥] and Robin Walsh*,[‡]

Contribution from the Instituto de Quimica-Fisica "Rocasolano", C.S.I.C., C/Serrano 119, 28006 Madrid, Spain, the School of Chemistry, University of Reading, Whiteknights, Reading, RG6 6AD, U.K.; Dow Corning Corporation, Mail Stop 128, 2200 West Saltzburg Road, P.O. Box 994, Midland, Michigan, 48686-0994, and the Department of Chemistry, University of Southampton, Highfield, Southampton, SO17 1BJ, U.K.

Received February 4, 2004; E-mail: r.walsh@reading.ac.uk

Abstract: Time-resolved kinetic studies of the reaction of silylene, SiH₂, with H₂O and with D₂O have been carried out in the gas phase at 297 K and at 345 K, using laser flash photolysis to generate and monitor SiH₂. The reaction was studied independently as a function of H₂O (or D₂O) and SF₆ (bath gas) pressures. At a fixed pressure of SF₆ (5 Torr), [SiH₂] decay constants, k_{obs}, showed a quadratic dependence on [H₂O] or [D₂O]. At a fixed pressure of H₂O or D₂O, k_{obs} values were strongly dependent on [SF₆]. The combined rate expression is consistent with a mechanism involving the reversible formation of a vibrationally excited zwitterionic donor−acceptor complex, H₂Si···OH₂ (or H₂Si···OD₂). This complex can then either be stabilized by SF₆ or it reacts with a further molecule of H₂O (or D₂O) in the rate-determining step. Isotope effects are in the range 1.0−1.5 and are broadly consistent with this mechanism. The mechanism is further supported by RRKM theory, which shows the association reaction to be close to its third-order region of pressure (SF₆) dependence. Ab initio quantum calculations, carried out at the G3 level, support the existence of a hydrated zwitterion H₂Si···(OH₂)₂, which can rearrange to hydrated silanol, with an energy barrier below the reaction energy threshold. This is the first example of a gas-phase-catalyzed silylene reaction.

Introduction

Silylenes are of importance because they are implicated in the thermal and photochemical breakdown mechanisms of silicon hydrides and organosilanes, as well as being key intermediates in chemical vapor deposition (CVD). Time-resolved kinetic studies, carried out over the past 15 years, have shown that the simplest silylene, SiH₂, reacts rapidly and efficiently with many chemical species.[1,2] Examples of its reactions include Si−H bond insertions, C=C and C≡C π-bond additions,[3] and reactions with lone pair donors such as ethers and alcohols.[3] This last category is of particular importance because it leads to formation of the Si−O bond, the key linkage in silicone polymers. As part of our investigations of the gas-phase reactions of SiH₂,[4−19] we recently investigated the kinetics of the prototype O-donor reaction of SiH₂ with H₂O.[19]

This reaction, already studied experimentally by Alexander et al.[20] and theoretically by Heaven et al.,[21] was found to be a pressure-dependent, third-body assisted association process, consistent with the reversible formation of a zwitterionic donor acceptor complex, viz.,

---

[†] Instituto "Rocasolano".
[‡] University of Reading.
[§] Dow Corning.
[∥] University of Southampton.
(1) Jasinski, J. M.; Becerra, R.; Walsh, R. *Chem. Rev.* **1995**, *95*, 1203.
(2) Becerra, R.; Walsh, R. Kinetics & mechanisms of silylene reactions: A prototype for gas-phase acid/base chemistry. In *Research in Chemical Kinetics*; Compton, R. G., Hancock, G., Eds.; Elsevier: Amsterdam, 1995; Vol. 3, p 263.
(3) Gaspar, P. P.; West, R. Silylenes. In *The Chemistry of Organic Silicon Compounds*; Rappoport, Z., Apeloig, Y., Eds.; Wiley: Chichester, U.K. 1998; Vol. 2, Chapter 43, p 2463.

(4) Becerra, R.; Frey, H. M.; Mason, B. P.; Walsh, R. *Chem. Phys. Lett.* **1991**, *185*, 415.
(5) Becerra, R.; Walsh, R. *Int. J. Chem. Kinet.* **1994**, *26*, 45.
(6) Al-Rubaiey, N.; Walsh, R. *J. Phys. Chem.* **1994**, *98*, 5303.
(7) Becerra, R.; Frey, H. M.; Mason, B. P.; Walsh, R.; Gordon, M. S. *J. Chem. Soc., Faraday Trans.* **1995**, *91*, 2723.
(8) Becerra, R.; Frey, H. M.; Mason, B. P.; Walsh, R. *J. Organomet. Chem.* **1996**, *521*, 343.
(9) Al-Rubaiey, N.; Carpenter, I. W.; Walsh, R.; Becerra, R.; Gordon, M. S. *J. Phys. Chem. A* **1998**, *102*, 8564.
(10) Becerra, R.; Boganov, S. E.; Walsh, R. *J. Chem. Soc., Faraday Trans.* **1998**, *94*, 3569.
(11) Becerra, R.; Walsh, R. *Int. J. Chem. Kinet.* **1999**, *31*, 393.
(12) Becerra, R.; Cannady, J. P.; Walsh, R. *J. Phys. Chem. A* **1999**, *103*, 4457.
(13) Becerra, R.; Carpenter, I. W.; Gutsche, G. J.; King, K. D.; Lawrance, W. D.; Staker, W. S.; Walsh, R. *Chem. Phys. Lett.* **2001**, *333*, 83.
(14) Becerra, R.; Cannady, J. P.; Walsh, R. *J. Phys. Chem. A* **2001**, *105*, 1897.
(15) Becerra, R.; Cannady, J. P.; Walsh, R. *Phys. Chem. Chem. Phys.* **2001**, *3*, 2343.
(16) Becerra, R.; Cannady, J. P.; Walsh, R. *J. Phys. Chem. A* **2002**, *106*, 4922.
(17) Al-Rubaiey, N.; Becerra, R.; Walsh, R. *Phys. Chem. Chem. Phys.* **2002**, *4*, 5072.
(18) Becerra, R.; Cannady, J. P.; Walsh, R. *J. Phys. Chem. A* **2002**, *106*, 11558.
(19) Becerra, R.; Cannady, J. P.; Walsh, R. *J. Phys. Chem. A* **2003**, *107*, 11049.
(20) Alexander, U. N.; King, K. D.; Lawrance, W. D. *J. Phys. Chem. A* **2002**, *106*, 973.
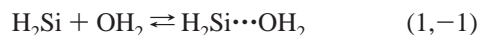(21) Heaven, M. W.; Metha, G. F.; Buntine, M. A. *J. Phys. Chem. A* **2001**, *105*, 1185.

$$H_2Si + OH_2 \rightleftarrows H_2Si\cdots OH_2 \qquad (1,-1)$$

The simplicity of this process is consistent with most of the kinetic measurements (but see below), the isotope effects, modeling by RRKM theory, and quantum chemical calculations which showed that a substantial energy barrier prevents the rearrangement of the complex to silanol, viz.,

$$H_2Si\cdots OH_2 \rightarrow H_3SiOH$$
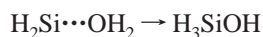
Similar findings have been obtained for the reactions of SiH_2 with MeOH and Me_2O.[13,22] The conclusion of these gas phase studies (and theory) is that the reaction effectively stops at the zwitterion stage, viz., that the zwitterion is the actual reaction product. The idea of such species as intermediates in reactions of silylenes with O-donor molecules goes back to the 1980s and the solution studies of Weber's group.[23-25] It is clear that in solution the zwitterions find ways to react further, and the solvent plays an important role. In the gas phase, the ultimate fate of the zwitterions is unclear. Possibilities include a wall reaction or a gas-phase-catalyzed reaction, which are too slow to affect the rate measurements on the fast (microsecond) time scale of laser flash photolysis experiments by ourselves[13,19] and others.[20,22] Bearing in mind these considerations, we were aware that in our earlier study[19] of $SiH_2 + H_2O$ (D_2O) there was evidence that rates measured at the lowest overall pressures (10 Torr) were too fast to be explained by the third-body-assisted association process. We thus decided to reinvestigate this gas-phase reaction under conditions that might reveal the presence of additional mechanistic contributions to the rate. We also decided to undertake further quantum chemical calculations to assist the interpretation of these experiments.

Experimental Section

Equipment, Chemicals, and Method. The apparatus and equipment for these studies have been described in detail previously.[7,26] Only essential and brief details are therefore included here. SiH_2 was produced by the 193-nm flash photolysis of phenylsilane ($PhSiH_3$) using a Coherent Compex 100 exciplex laser. Photolysis pulses were fired into a variable temperature quartz reaction vessel with demountable windows, at right angles to its main axis. SiH_2 concentrations were monitored in real time by means of a Coherent 699-21 single-mode dye laser pumped by an Innova 90-5 argon ion laser and operating with Rhodamine 6G. The monitoring laser beam was multipassed between 32 and 40 times along the vessel axis, through the reaction zone, to give an effective path length of up to 1.6 m. A portion of the monitoring beam was split off before entering the vessel for reference purposes. The monitoring laser was tuned to 17 259.50 cm^{-1}, corresponding to a known strong vibration–rotation transition[26,27] in the SiH_2 $A(^1B_1) \leftarrow X(^1A_1)$ absorption band. Light signals were measured by a dual photodiode/differential amplifier combination, and signal decays were stored in a transient recorder (Datalab DL910) interfaced to a BBC microcomputer. This was used to average the decays of between 5 and 20 photolysis laser shots (at a repetition rate of 0.5 or 1 Hz). The averaged decay traces were processed by fitting the data to an exponential form using a nonlinear least squares package. This analysis provided the values for first-order rate coefficients, k_{obs}, for removal of SiH_2 in the presence of known partial pressures of substrate gas.

Gas mixtures for photolysis were made up, containing between 1.0 and 4.3 mTorr of $PhSiH_3$, 0–12 Torr of H_2O (or D_2O), and inert diluent (SF_6) at added pressures of between 5 and 400 Torr. Pressures were measured by capacitance manometers (MKS, Baratron).

All gases used in this work were frozen at 77 K and pumped free of any vestiges of air prior to use. $PhSiH_3$ (99.9%) was obtained from Ventron-Alfa (Petrarch). H_2O (99.99%) was from local supply softened and demineralized, and D_2O (99.9%) was from Aldrich. Sulfur hexafluoride, SF_6, (no GC-detectable impurities) was from Cambrian Gases.

Ab Initio Calculations. The electronic structure calculations were performed with the Gaussian 98 software package.[28] All structures were determined by energy minimization at the MP2 = full/6-31G(d) level. Transition-state structures were characterized as first-order saddle points by calculation of the Hessian matrix. Stable structures, corresponding to energy minima, were identified by possessing no negative eigenvalues of the Hessian, while transition states were identified by having one and only one negative eigenvalue. The standard Gaussian-3 (G3) compound method[29] was employed to determine final energies for all local minima. For transition states the elements of the G3 method were used, viz., optimization to TS at HF/6-31G(d), frequencies at HF/6-31G(d), optimization to TS at MP2 = full/6-31G(d), followed by four single-point energy determinations at the MP2 = full/6-31G(d) geometry, viz., QCISD(T)/6-31G(d), MP4/6-31+G(d), MP4/6-31G(2df,p), and MP2 = full/G3large, and the values were combined according to the G3 procedure.[29] The identities of the transition-state structures were verified by calculation of intrinsic reaction coordinates[30] (IRC) at the MP2 = full/6-31G(d) or B3LYP/6-31G(d) levels. Reaction barriers were calculated as differences in G3 enthalpies at 298.15 K.

Results

Kinetic Measurements and Data Processing. Preliminary experiments established that, for a given reaction mixture, decomposition decay constants, k_{obs}, were not dependent on the exciplex laser energy (50–70 mJ/pulse, routine variation) or number of photolysis shots (up to 20 shots). The constancy of k_{obs} (five shot averages) showed no effective depletion of reactants. Higher pressures of precursor were required at the higher temperature because signal intensities decreased with increasing temperature. At each temperature the precursor pressure was kept fixed. In the previous investigation,[19] substrate pressures (H_2O or D_2O) were varied in the range 0–11 Torr, at each of a set of total pressures of 10, 30, 100, and 200 Torr, using SF_6 as bath gas (diluent). The extracted second-order rate constants showed a strong overall pressure dependence. However, the comparison of these results with RRKM theoretical expectations suggested that, at the total pressure of 10 Torr, and to a lesser extent at 30 Torr, the rate constant values might be too high. In these earlier experiments, because the reaction mixtures contained a sizable pressure of H_2O (or D_2O), the

(22) Alexander, U. N.; King, K. D.; Lawrance, W. D. *Phys. Chem. Chem. Phys.* **2001**, *3*, 3085.
(23) Steele, K. P.; Weber, W. P. *J. Am. Chem. Soc.* **1980**, *102*, 6095.
(24) Steele, K. P.; Weber, W. P. *Inorg. Chem.* **1981**, *20*, 1302.
(25) Steele, K. P.; Tzeng, D.; Weber, W. P. *J. Organomet. Chem.* **1982**, *231*, 291.
(26) Baggott, J. E.; Frey, H. M.; King, K. D.; Lightfoot, P. D.; Walsh, R.; Watts, I. M. *J. Phys. Chem.* **1988**, *92*, 4025.
(27) Jasinski, J. M.; Chu, J. O. *J. Chem. Phys.* **1988**, *88*, 1678.

(28) Frisch, M. J.; Trucks, G. W.; Schlegel, H. B.; Scuseria, G. E.; Robb, M. A.; Cheeseman, J. R.; Zakrzewski, V. G.; Montgomery, Jr., J. A.; Stratmann, R. E.; Burant, J. C.; Dapprich, S.; Millam, J. M.; Daniels, A. D.; Kudin, K. N.; Strain, M. C.; Farkas, O.; Tomasi, J.; Barone, V.; Cossi, M.; Cammi, R.; B. Mennucci, B.; Pomelli, C.; Adamo, C.; Clifford, S.; Ochterski, J.; Petersson, G. A.; Ayala, P. Y.; Cui, Q.; Morokuma, K.; Malick, D. K.; Rabuck, A. D.; Raghavachari, K.; Foresman, J. B.; Cioslowski, J.; Ortiz, J. V.; Baboul, A. G.; Stefanov, B. B.; Liu, G.; Liashenko, A.; Piskorz, P.; Komaromi, R.; Gomperts, R.; Martin, R. L.; Fox, D. J.; Keith, T.; Al-Laham, M. A.; Peng, C. Y.; Nanayakkara, A.; Gonzales, C.; Challacombe, M.; Gill, P. M. W.; Johnson, B. G.; Chen, W.; Wong, M. W.; Andres, J. L.; Head-Gordon, M.; Replogle, E. S.; Pople, J. A. *Gaussian 98*, Revision A.9; Gaussian Inc.: Pittsburgh, PA, 1998.
(29) Curtiss, L. A.; Raghavachari, K.; Redfern, P. C.; Rassolov, V.; Pople, J. A. *J. Chem. Phys.* **1998**, *109*, 7764.
(30) Gonzales, C.; Schlegel, H. B. *J. Chem. Phys.* **1989**, *90*, 2154.

Table 1. Rate Constants Obtained by Fitting[a,b] Experimental Decay Data to Quadratic Eq X at Constant SF$_6$ (5 Torr)

		$k_a/10^4$ s^{-1}	$k_b/10^{-13}$ cm^3 molecule^{-1} s^{-1}		$k_c/10^{-30}$ cm^6 molecule^{-2} s^{-1}	
reaction	temp/K	best fit[a,b]	best fit[a]	fixed[c]	best fit[a]	constrained[b]
SiH$_2$ + H$_2$O	297	3.14 ± 1.04	(7.9 ± 2.8)	3.72	(3.8 ± 1.4)	6.0 ± 0.4
SiH$_2$ + H$_2$O	345	3.20 ± 0.36	(2.1 ± 0.7)	0.955	(2.6 ± 0.3)	2.95 ± 0.09
SiH$_2$ + D$_2$O	297	2.91 ± 0.60	(5.4 ± 1.7)	3.55	(4.5 ± 0.9)	5.4 ± 0.2
SiH$_2$ + D$_2$O	345	4.64 ± 0.74	(2.1 ± 1.1)	0.759	(1.8 ± 0.4)	2.20 ± 0.09

[a] Least squares best fit to all three rate constants. [b] Best fit with k_b fixed (see text): values for k_a almost unchanged and therefore not listed. [c] k_b values uncertain by ca. ±15% from theoretical extrapolation.
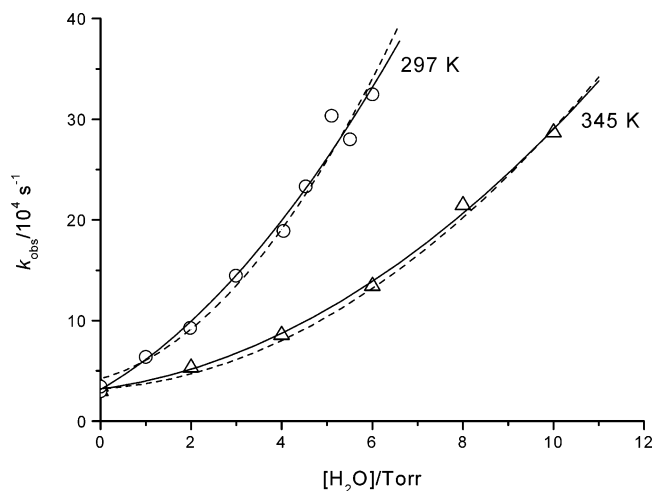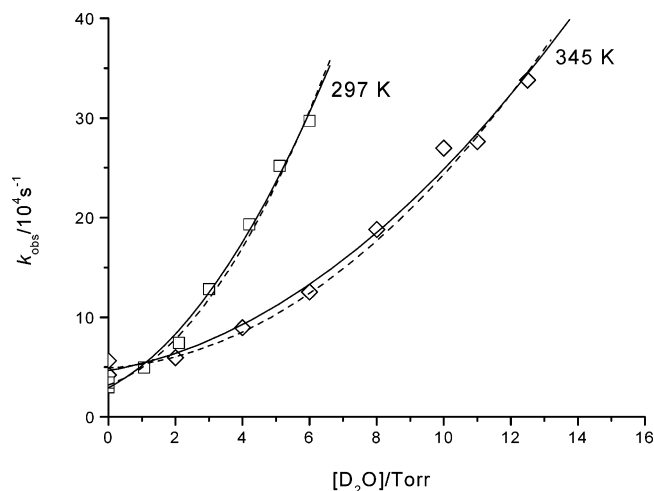

Figure 1. Dependence of decay constants on [H$_2$O] at 5 Torr SF$_6$ partial pressure. Data points: ○ 297 K, △ 345 K. Lines of fit: best fit (—), constrained fit (− − −).

Figure 2. Dependence of decay constants on [D$_2$O] at 5 Torr SF$_6$ partial pressure. Data points: □ 297 K, ◇ 345 K, Lines of fit: best fit (—), constrained fit (− − −).

proportion of SF$_6$ in the reaction mixtures varied significantly as the substrate was varied. Thus, if the stabilizing efficiencies of H$_2$O (or D$_2$O) and SF$_6$ are different in this reaction system, then, under the conditions of the previous study, the variations in substrate pressure would have caused variations in third body stabilization effects, the consequences of which could not be separated. Thus, in the present study, experiments were carried out first under conditions of constant SF$_6$ and second under conditions of constant H$_2$O (or D$_2$O).

(i) Experiments at constant SF$_6$ (5 Torr). For each system (either SiH$_2$ + H$_2$O or SiH$_2$ + D$_2$O), a series of experiments was carried out in which the substrate pressure was varied from 0 to 6 Torr (at 297 K) and 0 to 12 Torr (at 345 K). The results of these experiments are shown in Figures 1 and 2. These figures clearly demonstrate the nonlinear dependence of k_{obs} with substrate pressure (for both H$_2$O and D$_2$O). This is the first example of such a nonlinear dependence for a gas-phase silylene reaction. The data were fitted, by nonlinear least squares, to a three-term polynomial (i.e., quadratic) equation, viz.,

$$k_{obs} = k_a + k_b[\text{H}_2\text{O}] + k_c[\text{H}_2\text{O}]^2 \qquad (X)$$

Examination of Figures 1 and 2 shows that the fit to the data is good in all cases. The values obtained for the constants k_a, k_b, and k_c are shown in Table 1. The error limits are single standard deviations and show significant uncertainties, particularly in the values for k_b. However, with polynomial fits, the greater the number of variable terms, the higher the correlation between the values of the coefficients (i.e., the constants). We can take advantage of these correlations to show that with a somewhat altered, but constrained, set of values for k_b, reasonable fits to

the data can still be obtained. This further processing of the data is described below after the next section.

(ii) Experiments at constant substrate pressure. In these experiments, the H$_2$O (or D$_2$O) pressure was fixed at 2.0 Torr at 297 K and at 4.0 Torr at 345 K. Then, for each reaction system, at each temperature, a series of runs was carried out in which SF$_6$ pressures were varied between 10 and ca. 100 Torr. The results of these experiments were processed as follows. It was assumed that eq X applied. The measured k_{obs} values were used to obtain k_{obs}' via eq Y or its D$_2$O equivalent:

$$k_{obs}' = k_{obs} - k_a - k_c[\text{H}_2\text{O}]^2 \qquad (Y)$$

The values used for k_a and k_c were those derived from the initial data fitting shown in Table 1, which were assumed not to be pressure (i.e., [SF$_6$]) dependent. The values for k_b were then calculated from eq Z or its D$_2$O equivalent:

$$k_b = k_{obs}'/[\text{H}_2\text{O}] \qquad (Z)$$

The results of these experiments (values of k_{obs}, k_{obs}', and k_b at each SF$_6$ pressure) are shown in Tables 2 and 3. It can be clearly seen that k_b is significantly pressure-dependent. It is shown below that k_b represents the normal bimolecular association rate constant for this reaction system, and therefore its pressure dependence here corresponds to that for the third-body effect of SF$_6$ alone. Tables 2 and 3 show that the effect of correction for the intercept (k_a) and for the quadratic term ($k_c[\text{H}_2\text{O}]^2$), i.e., the conversion of k_{obs} to k_{obs}', while relatively small, is still proportionately largest at low values of [SF$_6$]. This systematic pressure dependence of k_b allows us to refine the fitting to the quadratic eq X. This is described in the next section.

Table 2. Experimental Decay Constants, Corrected Decay Constants,[a] and Refined Values for Second-Order Rate Constants, k_b, for $SiH_2 + H_2O$, as a Function of SF_6 Pressure

[SF₆]/Torr	$k_{obs}/10^4\ s^{-1}$	$k_{obs}'/10^4\ s^{-1\ b}$	$k_b/10^{-12}\ cm^3\ molecule^{-1}\ s^{-1\ b}$
$SiH_2 + H_2O$ at 297 K ([H₂O] = 2 Torr)			
10	10.3	4.6 (5.5)	0.71 (0.85)
22.5	14.1	8.4 (9.3)	1.29 (1.43)
28	17.2	11.5 (12.4)	1.76 (1.90)
30	16.7	11.0 (11.9)	1.69 (1.83)
40	21.0	15.3 (16.2)	2.35 (2.49)
50	22.9	17.2 (18.1)	2.65 (2.78)
73	26.6	20.9 (21.8)	3.21 (3.34)
91	31.3	25.6 (26.5)	3.94 (4.08)
104	35.2	29.5 (30.4)	4.54 (4.67)
$SiH_2 + H_2O$ at 345 K ([H₂O] = 4 Torr)			
12	11.5	2.9 (3.4)	0.26 (0.30)
20	12.0	3.4 (3.9)	0.30 (0.34)
30	14.0	5.4 (5.9)	0.48 (0.53)
40	15.5	6.9 (7.4)	0.61 (0.66)
60	19.3	10.7 (11.2)	0.96 (1.00)
82	23.8	15.2 (15.7)	1.36 (1.40)
105	26.6	18.0 (18.5)	1.61 (1.65)

[a] Corrected for contribution of k_a and $k_c[H_2O]^2$ (see text). [b] First round values are in parentheses i.e., values before final correction (see text).

Table 3. Experimental Decay Constants, Corrected Decay Constants,[a] and Refined Values for Second-Order Rate Constants, k_b, for $SiH_2 + D_2O$, as a Function of SF_6 Pressure

| [SF₆]/Torr	$k_{obs}/10^4\ s^{-1}$	$k_{obs}'/10^4\ s^{-1\ b}$	$k_b/10^{-12}\ cm^3\ molecule^{-1}\ s^{-1\ b}$
$SiH_2 + D_2O$ at 297 K ([D₂O] = 2 Torr)			
8	8.6	3.1 (3.5)	0.47 (0.53)
20	13.1	7.6 (8.0)	1.17 (1.23)
30	16.7	11.2 (11.6)	1.72 (1.79)
50	22.7	17.2 (17.6)	2.64 (2.72)
60	24.4	18.9 (19.3)	2.90 (2.97)
65.5	22.3	16.8 (17.2)	2.58 (2.65)
75	29.0	23.5 (23.9)	3.61 (3.69)
85	34.1	28.6 (29.0)	4.39 (4.47)
96	34.8	29.3 (29.7)	4.51 (4.58)
$SiH_2 + D_2O$ at 345 K ([D₂O] = 4 Torr)			
21.5	9.6	1.9 (2.4)	0.17 (0.21)
30	11.7	4.0 (4.5)	0.36 (0.40)
50.5	15.4	7.7 (8.2)	0.69 (0.73)
67	15.4	7.7 (8.2)	0.69 (0.73)
80	18.8	11.1 (11.6)	0.99 (1.04)
112	21.4	13.7 (14.2)	1.22 (1.27)

[a] Corrected for contribution of k_a and $k_c[D_2O]^2$ (see text). [b] First-round values are in parentheses, i.e., values before final correction (see text).

(iii) **Further refinement of the rate constants.** The pressure-dependent k_b values were extrapolated to 5 Torr SF_6, assuming a close to linear pressure dependence (see later). This gave another set of k_b values also shown in Table 1. These values were then employed as fixed constants in eq X, and fitting was reoptimized (using least-squares procedures, as described in section (i)) to obtain new values for k_c. These are also shown in Table 1. The comparison of the fit to the original data using eq X with these new constants is also shown in Figures 1 and 2. The quality of fit is hardly affected, and it can be seen to be not much worse than the original and well within the uncertainties of the raw data. It is justified by the fact that the mechanistic model (see next section) leads us strongly to believe in the revealed pressure-dependent trend of k_b. With the new values for k_c, further small improvements in the values for k_b were then calculated, using the same procedure described in section (ii). These new values are shown in Tables 2 and 3 alongside earlier ones. No further refinement was undertaken beyond this cycle.

Table 4. Some Directly Obtained Second-Order Rate Constants for $SiH_2 + H_2O$ and D_2O at 297 and 345 K at Higher Pressures

P/Torr	k (H₂O)[a]	k (D₂O)[a]	k_H/k_D
T = 297 K			
100	5.10 ± 0.19	4.44 ± 0.14	1.149 ± 0.056
200	6.76 ± 0.24	6.61 ± 0.56	1.023 ± 0.093
400	10.49 ± 1.32	14.82 ± 1.54	0.71 ± 0.12
T = 345 K[b]			
100	1.92 ± 0.14	1.80 ± 0.04	1.066 ± 0.081
200	3.33 ± 0.24	2.90 ± 0.12	1.148 ± 0.095
400	3.76 ± 0.24	3.90 ± 0.28	0.96 ± 0.14

[a] Units: $10^{-12}\ cm^3\ molecule^{-1}\ s^{-1}$. [b] Original 100 and 200 Torr measurements were made at 339 K. No corrections have been made for this.
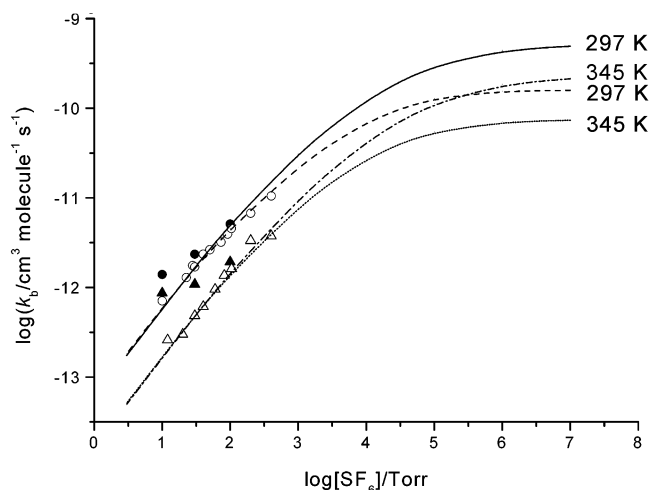
Figure 3. Pressure dependence of the second-order rate constants, k_b, for $SiH_2 + H_2O$. At 297 K, ○ (this work), ● (ref 19). At 345 K, △ (this work), ▲ (ref 19). Lines are RRKM fits corresponding to different transition states: TSa (—,—·—·), TSb (− − −, ····). See text for details.

(iv) **High-pressure measurements.** To extend the range of SF_6 pressure as far as practicable, we carried out one further set of experiments at 400 Torr total pressure. In these experiments, the pressures of H_2O and D_2O were so small (less than 0.7 Torr at 297 K and 2.0 Torr at 345 K) that corrections for the quadratic term, $k_c[H_2O]^2$, were negligible and plots of k_{obs} against [H₂O] (or [D₂O]) were effectively linear with gradients equal to k_b and represent the normal second-order rate constants. The values obtained are shown in Table 4 together with those obtained previously[19] at 100 and 200 Torr total pressure. This set of results, showing the sharp increase in second-order rate constant values, emphasizes the significant pressure dependence in k_b extends to higher pressures than those explored previously.[19] Higher pressures could not be investigated because above 400 Torr the SiH_2 signals were largely quenched and reliable decays were difficult to obtain. The dependence of the second-order rate constants (k_b) for the $SiH_2 + H_2O$ system, on SF_6 pressure over the full range, is shown in Figure 3. This also shows earlier experimental values and the results of Rice, Ramsperger, Kassel, Marcus (RRKM) calculations[31] for two different transition-state models (see next section). The SF_6 pressure dependences for $SiH_2 + D_2O$ were very similar and are not shown.

As well as showing that the rate constants increase with increasing pressure, these results also show that they decrease

(31) Holbrook, K. A.; Pilling, M. J.; Robertson, S. H. *Unimolecular Reactions*, 2nd ed.; Wiley: Chichester, U.K., 1996.
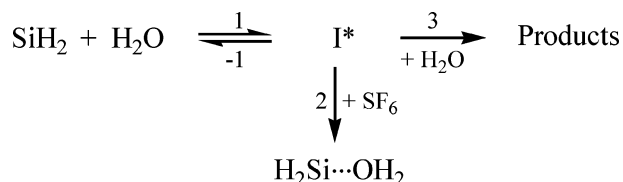
Table 5. Molecular and Transition-State Parameters for RRKM Calculations for Decomposition of the $H_2Si\cdots OH_2$ Adduct

		TS complex[a]			
parameter	molecule[a]	TSa(297 K)	TSa(345 K)	TSb(297 K)	TSb(345 K)
O—H str(2)	3715	3715	3715	3715	3715
	3613	3613	3613	3613	3613
Si—H str(2)	1965	1965	1965	1965	1965
	1918	1918	1918	1918	1918
OH_2 bend	1611	1611	1611	1611	1611
SiH_2 bend	997	997	997	997	997
Si—O str	776	rxn coord	rxn coord	rxn coord	rxn coord
OH_2 wag	509	102	120	180	190
OH_2 rock	408	100	105	150	150
SiH_2 wag	651	130	130	200	235
SiH_2 rock	257	70	75	100	110
Si$\cdots$O torsion	154	40	45	75	80
A/s^{-1}		1.0×10^{16}	9.0×10^{15}	1.0×10^{15}	9.0×10^{14}
E_o/kJ mol^{-1}		65	65	54	54
$Z/10^{-10}$ cm^3 molecule^{-1} s^{-1}		4.38	4.47	4.38	4.47

[a] Wavenumbers in cm^{-1}.

with temperature (just as has been found in similar SiH_2 association reactions[5−7,9,12,14,15,17]). In this study, the rate measurements were limited to two temperatures, viz., 297 and 345 K. At higher temperatures the quality of the reaction decay traces became poorer (signal decays not exponential with slow return to baseline). This is probably due to the onset of reversibility, as observed by AKL in the SiH_2 + MeOH[20] and SiH_2 + Me_2O[22] reaction systems. The temperature range of 48 K is insufficient to obtain reliable Arrhenius parameters, but from the average decrease in rate constant between 297 and 345 K, an activation energy of ca −21 (± 3) kJ mol^{-1} is calculated.

Mechanistic Treatment. The kinetic results obtained here suggest a pressure-dependent association reaction combined with a process affected by an additional water molecule. The following mechanism is proposed as a working hypothesis:

$$SiH_2 + H_2O \underset{-1}{\overset{1}{\rightleftharpoons}} I^* \overset{3}{\underset{+ H_2O}{\longrightarrow}} \text{Products}$$
$$2 \downarrow + SF_6$$
$$H_2Si\cdots OH_2$$

I* represents the vibrationally excited donor−acceptor adduct, $H_2Si\cdots OH_2^*$. Assuming I* is at steady state, then:

$$k_1[SiH_2][H_2O] = k_{-1}[I^*] + k_2[I^*][SF_6] + k_3[I^*][H_2O]$$

which gives:

$$[I^*] = k_1[SiH_2][H_2O]/\{k_{-1} + k_2[SF_6] + k_3[H_2O]\} \quad (A1)$$

The observed first-order decay constant is given by:

$$k_{obs}[SiH_2] = -d[SiH_2]/dt = k_2[I^*][SF_6] + k_3[I^*][H_2O] \quad (A2)$$

Combination of A1 and A2 gives

$$k_{obs} = k_1[H_2O]\frac{k_2[SF_6] + k_3[H_2O]}{k_{-1} + k_2[SF_6] + k_3[H_2O]} \quad (A3)$$

Under conditions where redissociation of I* is predominant, $k_{-1} \gg (k_2[SF_6] + k_3[H_2O])$ and eq A3 reduces to:

$$k_{obs} = k_2\left(\frac{k_1}{k_{-1}}\right)[H_2O][SF_6] + k_3\left(\frac{k_1}{k_{-1}}\right)[H_2O]^2 \quad (A4)$$

This result matches the empirical eq X, where the fitted rate constants correspond as follows:

$$k_b = k_2\left(\frac{k_1}{k_{-1}}\right)[SF_6], \quad k_c = k_3\left(\frac{k_1}{k_{-1}}\right)$$

The fitted constant k_a corresponds to the loss process of SiH_2 with precursor, which was not included in the above analysis for simplicity. The conditions under which eq A4 is applicable correspond to the low pressure limit of the association reaction. This is discussed in the next section.

RRKM Calculations. The procedures,[31] the description of transition states, and collision deactivation models were described in detail previously,[19] and therefore, only essential and brief details are given here. The objective was to model the SF_6 pressure dependence of the bimolecular association process (steps 1, −1, and 2 of the mechanism). This will have the same SF_6 pressure dependence as the reverse dissociation process, viz.,

$$H_2Si\cdots OH_2 \rightarrow SiH_2 + H_2O$$
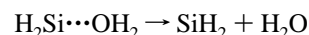
From thermodynamic considerations ($\Delta S°$) and kinetic arguments, the A factors for two potential transition states TSa and TSb were derived. The vibrational assignments of $H_2Si\cdots OH_2$, TSa, and TSb were made on the basis of the results of ab initio calculations carried out previously[19] and adjustments of key (transitional) wavenumbers to fit the A factors. Small modifications were made to both TSa and TSb to allow for the temperature change from 297 to 345 K. (Previously the temperatures of study were 296 and 339 K, but the vibrational assignments used here for 345 K were unaltered from those at 339 K.) Summaries of the salient features of the TS models are given in Table 5, including the critical energies which were also based on the ab initio calculations carried out previously.[19] The collisional deactivated process was based on a stepladder model with an energy removal parameter, $\langle \Delta E \rangle_{down}$ of 12.0 kJ mol^{-1} (1000 cm^{-1}).

The calculated pressure-dependence (falloff) curves are shown in Figure 3. The curves are positioned to match the data at the

pressures of study (as far as is possible). The comparison with experiment shows good fitting for both models at both temperatures. However, the two pairs of curves corresponding to TSa and TSb diverge significantly from one another at high pressures. Because the high pressure limiting values of the second-order rate constants, k_1^∞, for $SiH_2 + H_2O$ are not known, this cannot be used as a criterion to select which fit is best. We favor the tighter transition-state TSb for reasons given earlier[19] but recognize that this question cannot be settled until a way is found to probe the high pressure limit. (It is well-known to practioners in the field of unimolecular reactions[31] that transition-state descriptions cannot be obtained from low pressure limiting rate constants, where energy transfer controls the rate.) The pressure dependences found in the region $10-100$ Torr from these calculations, expressed as $[SF_6]^n$, correspond to values of n of 0.95 (TSa, 297 K), 0.96 (TSa, 345 K), 0.89 (TSb, 297 K), and 0.93 (TSb, 345 K). These values close to 1.0 show that with both models the reaction is approaching its low pressure (third order) limit of pressure dependence. This confirms the kinetic treatment of the mechanism leading to eq A4 and justifies the linear extrapolation used to obtain k_b values at 5 Torr during the data processing.

Ab Initio Calculations. The potential energy surface for the reaction of SiH_2 with H_2O was calculated by us earlier[19] using both G2 and G3 procedures. Our objective here was to see whether we could find structures and an energy surface for the reaction of SiH_2 with two molecules of H_2O which would correspond to the kinetic term, quadratic in H_2O, found experimentally. As hoped, we obtained at the G3 level a set of species corresponding closely to those found earlier[19] but of formula SiH_6O_2 rather than SiH_4O. Apart from the reactants and stable products ($SiH_3OH + H_2O$), there are five other stable species (or combinations of species), viz., (i) $H_2Si\cdots(OH_2)_2$, a complex of $SiH_2 + H_2O$ but associated with, and stabilized by, a further H_2O molecule, (ii) a hydrated silanol in two forms ($H_3SiO(H)\cdot\cdot HOH$ and $H_3SiOH\cdot\cdot OH_2$, where the associated H_2O molecule is H-bonded with either the O or (O)H in the silanol), the lowest energy species on the surface, and (iii) $H_2 + HSi$-$(OH)\cdots OH_2$ (a hydrated hydroxysilylene in both cis (c) and (t) forms). In addition, we have located seven transition states, viz., TS1 leading from $H_2Si\cdots(OH_2)_2$ to $H_3SiO(H)\cdots HOH$, TS2c/TS2t leading from $H_2Si\cdots(OH_2)_2$ to $H_2 + HSi(OH)\cdots$ OH_2 (c and t) via H_2 elimination, and TS3c(O··H)/TS3t(O··H) and TS3c(H··O)/TS3t(H··O) connecting either $H_3SiO(H)\cdots HOH$ or $H_3SiOH\cdot\cdot OH_2$ to $H_2 + HSiOH\cdots OH_2$ (c and t), also an H_2 elimination process. The transition states for H_2 elimination from $H_2Si\cdots(OH_2)_2$ and from $H_3SiO(H)\cdot\cdot HOH$ (or $H_3SiOH\cdot\cdot OH_2$) are clearly different from one another.

The structures of all species are shown in Figure 4, and their enthalpy values are listed in Table 6. This last table includes the lower level RHF and MP2 values as well as those at G3† to show how the latter performs compared with these lower levels of theory (†A reviewer who questioned the use of G3 for this system because it is a single-configurational method has in fact found, via a six-electron, five-orbital CASSCF/6-31G(d) calculation on TS2c, that a single determinant is a reasonable description; i.e., G3 is adequate.). While RHF and MP2 do relatively well compared to G3 for the stable species, only MP2 gives reasonable values compared to G3 for the transition states. The key species are represented on the potential energy
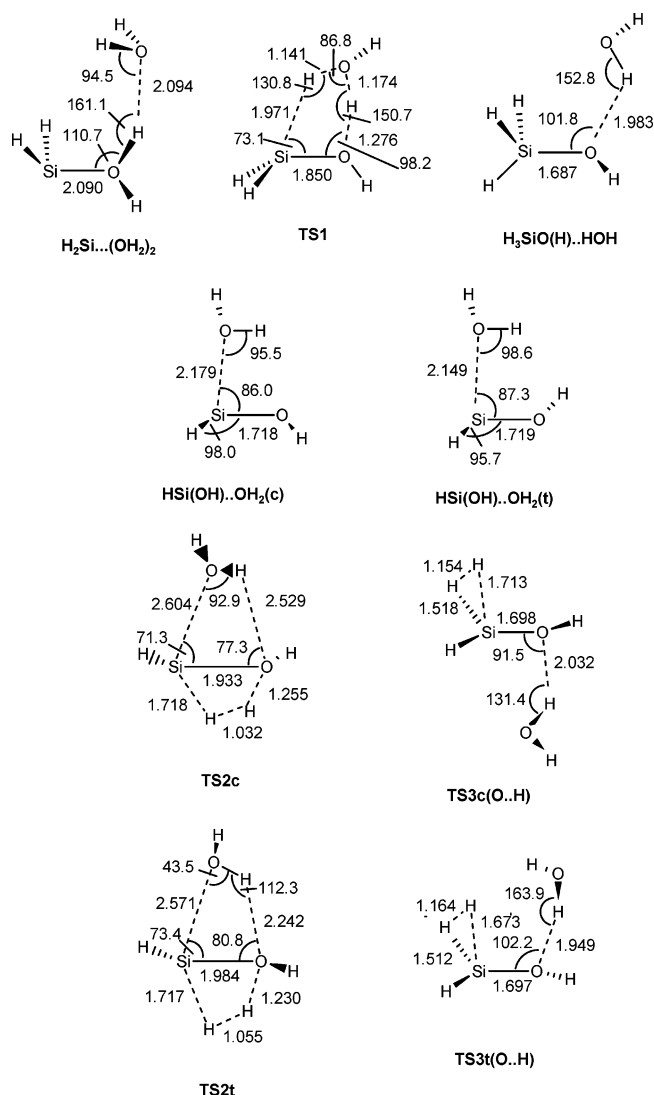

Figure 4. Ab initio MP2 = full/6-31G(d) calculated geometries of local minimum structures and transition states on the $SiH_2 + H_2O$ energy surface. Selected distances are given in angstroms, and angles are given in degrees.

(enthalpy) surface in Figure 5. For simplification and clarity, the species hydrated through the H-atom of the OH group in silanol (and its decomposition pathways) are not shown in this figure. The existence of this added pathway does not affect any conclusions. Other potential structures involving alternative H-bonding of the extra H_2O molecule were found not to be competitive (e.g., with TS2c/TS2t). Most of the structures found resemble their analogues on the SiH_4O surface,[19] but with an added hydrogen-bonded water molecule. On the energy surface, the key point to be noted is that TS1 lies below the threshold energy for reaction, thus making conversion of $SiH_2 + 2H_2O$ to $SiH_3OH + H_2O$ an energetically downhill process. In Figure 5, the direct elimination of H_2 by $H_2Si\cdots OH_2$ looks uncompetitive (TS2c/t lie well above TS1). The formation of $HSiOH\cdots$ OH_2 (c and t) via TS3, however, is energetically possible starting from $SiH_2 + 2H_2O$. Nevertheless, it seems more likely that, once formed, the silanol-water complex (either form) will simply lose H_2O, and despite the large energy release involved in formation of this complex, the residual SiH_3OH will not have enough energy to dissociate via TS3 (on the SiH_4O surface[19]). In Figure 4, many of the geometric details are omitted for the sake of clarity. It should be noted that the coordinating H_2O

Table 6. Ab Initio G3, RHF/6-31G(d), and MP2 = full/6-31G(d) Enthalpies for SiH$_6$O$_2$ Species of Interest in the SiH$_2$ + 2H$_2$O Reaction

molecular species	G3 enthalpy[a]	relative[b]	RHF[a,c]	relative[b]	MP2[a,d]	relative[b]
SiH$_2$ + 2H$_2$O	−443.210232	0	−441.959457	0	−442.413878	0
H$_2$Si···(OH$_2$)$_2$	−443.249325	−103	−441.994368	−92	−442.465232	−135
H$_3$SiO(H)···HOH	−443.330997	−317	−442.080126	−318	−442.545781	−346
H$_3$SiOH···OH$_2$	−443.334554	−326	−442.083648	−326	−442.549321	−356
H$_3$SiOH + H$_2$O	−443.326417	−305	−442.076024	−306	−442.537911	−326
H$_2$+HSi(OH)···OH$_2$(c)	−443.268728	−154	−442.009815	−132	−442.488991	−197
H$_2$ + HSi(OH)···OH$_2$(t)	−443.270280	−158	−442.010646	−134	−442.490518	−201
TS1	−443.232873	−59	−441.960571	−3	−442.451778	−99
TS2c	−443.211219	−3	−441.927027	+85	−442.415419	−4
TS2t	−443.209853	+1	−441.925166	+90	−442.414392	−1
TS3t(H···O)	−443.232691	−59	−441.944068	+40	−442.432879	−50
TS3t(O···H)	−443.230172	−52	−441.941111	+48	−442.428437	−38
TS3c(H···O)	−443.230313	−53	−441.941857	+46	−442.429768	−42
TS3c(O···H)	−443.234186	−63	−441.945154	+38	−442.433295	−51

[a] $H°$ (298 K) values in Hartrees. [b] Relative energy in kJ mol^{-1}. [c] RHF/6-31G(d). [d] MP2 = full/6-31G(d).
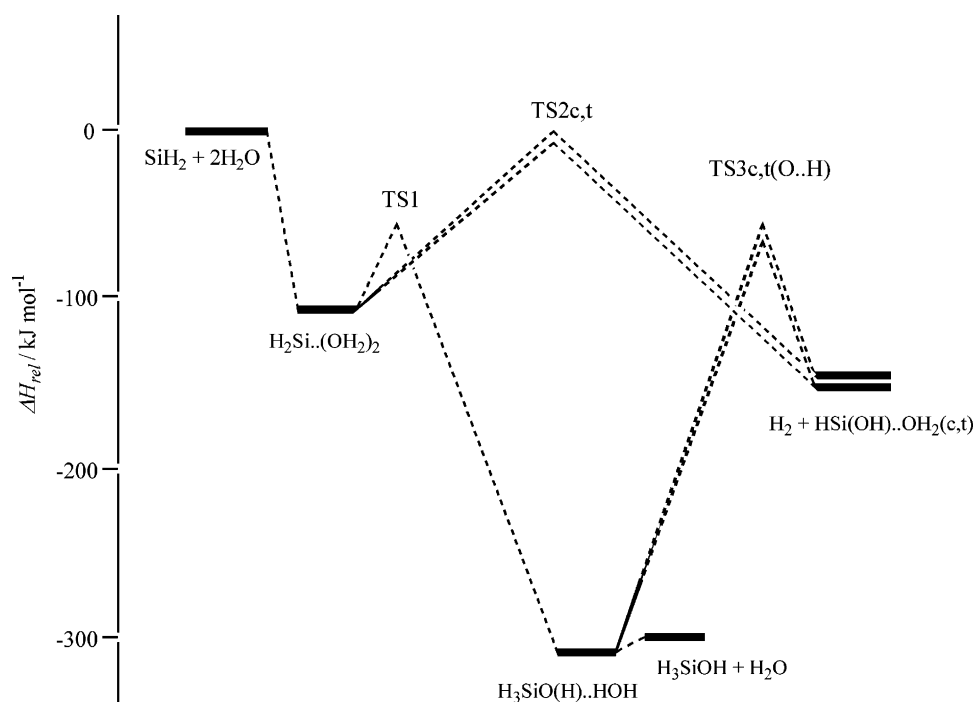
Figure 5. Potential energy (enthalpy) surface for the reaction of SiH$_2$ + 2H$_2$O. All enthalpies are calculated at the G3 level.

molecule is, for all structures except TS1, very close to having an unperturbed geometry (O−H bond length, 0.969−0.979 Å; HOH bond angle, 103.8−105.7°). The Si−H bonds have typical lengths (1.476−1.539 Å). Thus, the parameters marked in the structures are largely those defining the bond linkages between the hydrogen-bonded H$_2$O molecule and the rest of the molecular frame.

Discussion

General Comments, Kinetic Analysis, Isotope Effects, and Comparison of Results with RRKM Theory. The main experimental purpose of this study was to investigate the kinetics of the SiH$_2$ + H$_2$O and SiH$_2$ + D$_2$O reactions under low pressure conditions and to identify the additional contribution to the rate, over and above the third body assisted association reaction previously identified.[19] This has been accomplished, and a process second order in [H$_2$O] has been found. In the other previous study of this reaction, by Alexander et al.,[20] this process was not observed in the presence of argon, but the lowest pressure used was 50 Torr and its contribution would have been very small.

We have shown here that the decay process of SiH$_2$ with H$_2$O and D$_2$O can be separated into two terms, and that the kinetics are best understood in terms of a mechanism whereby the initially formed H$_2$Si···OH$_2$ complex (vibrationally excited) is either stabilized by SF$_6$ or reacts with a further molecule of H$_2$O. The best separation of the kinetic terms, although not providing the best overall fit to the data, has been shown to be very close to it. This is so because at 5 Torr of SF$_6$ the quadratic term in H$_2$O is dominant and the data are relatively insensitive to the value of k_b (even outside the uncertainty limits of the best fit values; see Table 1). The RRKM modeling, which shows an excellent fit to the SF$_6$ pressure dependence of k_b, was used to fix the value of k_b at 5 Torr and thereby constrain the values of k_c. The k_c values were all increased (see Table 1) and in one case (out of four) beyond the error limits of the best fit. The self-consistency of the data is shown by the relative third body efficiencies of H$_2$O and SF$_6$ (discussed in the next section) and by the isotope effects. In Table 1, the best fit values for k_b favor SiH$_2$ + H$_2$O over SiH$_2$ + D$_2$O at 297 K and show no difference at 345 K. For k_c SiH$_2$ + D$_2$O is faster at 297 K, whereas
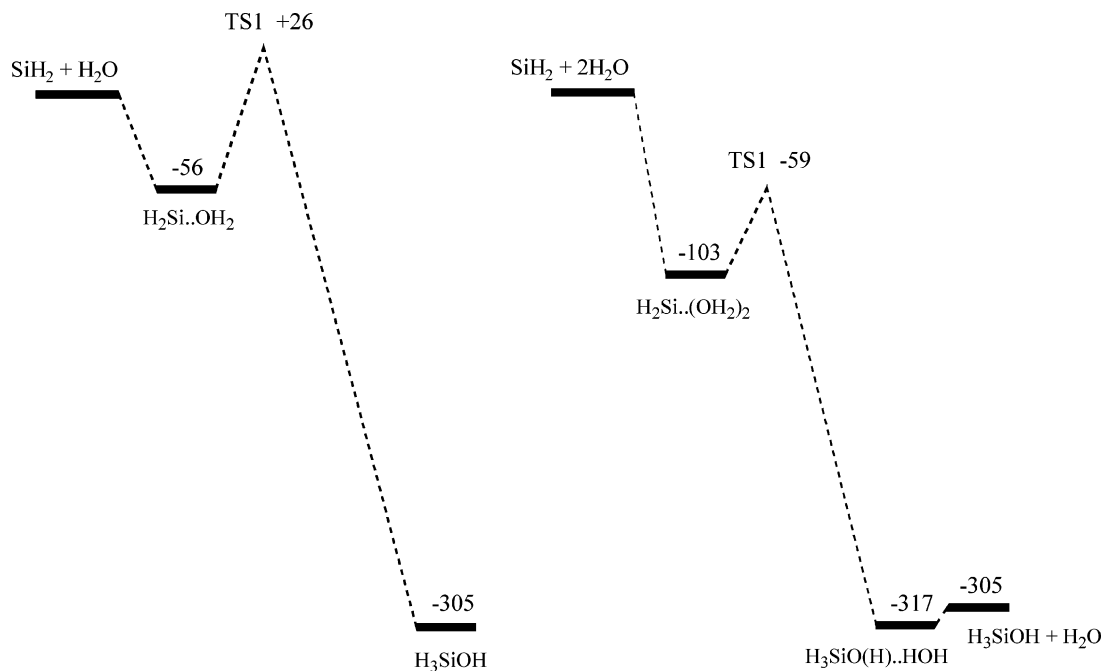
Figure 6. Comparison of parts of the G3 calculated PE surfaces for the $SiH_2 + H_2O$ (SiH_4O) and the $SiH_2 + 2H_2O$ (SiH_6O_2) systems. All energies in kJ mol^{-1}.

$SiH_2 + H_2O$ is faster at 345 K. For the fixed and constrained data, $SiH_2 + H_2O$ is favored consistently over $SiH_2 + D_2O$ for both k_b and k_c.

The isotope effects obtained previously[19] were quite small (1.076 ± 0.080) and independent of temperature and pressure. But of course since k_b and k_c were not separated previously, this may have hidden more significant effects. Although there is some scatter in the data, the effects seen in Tables 1−4 suggest a slightly more complex picture. For both k_b and k_c at 297 K, values of k_H/k_D appear to lie in the range 1.00−1.15 (apart for the 400 Torr (SF_6) data). At 345 K, k_{cH}/k_{cD} is 1.34 while values for k_{bH}/k_{bD} are SF_6 pressure-dependent, varying between 0.96 at 400 Torr to ca. 1.5 at 10 Torr. Certainly for the association reaction which does not involve the participation of a migrating H (or D) in the rate-determining step, values close to unity are to be expected. For k_c, relating to a process involving an additional molecule of H_2O (D_2O) the expectation is not clear. A more detailed analysis of the isotope effects is beyond the scope of the present work.

Our study was limited to two temperatures by problems of reversibility at higher temperatures. The negative temperature dependence of the $SiH_2 + H_2O$ reaction mirrors that of the $SiH_2 + CD_3OD$ reaction also studied by Alexander et al.[20] as well as that of many other silylene reactions studied in our laboratory.[5−7,9,12,14,15,17]

Figure 3 shows the comparison of the experimental values for k_b with both the previous values[19] (obtained when we had not considered the other contribution to the rate) and the RRKM models. Our analysis of the kinetics now clearly shows the significant reduction in values for the rate constants, now identified as k_b, at the lower SF_6 pressures, and also the markedly improved fit of experiment with theory. As can be clearly seen it is not possible to distinguish between TSa and TSb, even though we favor the latter. It is also not possible to rule out other transition states, incorporating partial rotational modes, as favored by Alexander et al.[20] This has been discussed in detail

Table 7. Third-Order (Limiting) Rate Constants for $SiH_2 + H_2O$ (and D_2O) at 297 and 345 K for SF_6 and H_2O as Third Bodies

		k/10^{-30} cm^6 molecule^{-2} s^{-1}	
reaction	temp/K	+ SF₆	+ H₂O
$SiH_2 + H_2O$	297	2.29	6.0
$SiH_2 + H_2O$	345	0.68	2.95
$SiH_2 + D_2O$	297	2.18	5.4
$SiH_2 + D_2O$	345	0.54	2.20

earlier[19] and is not repeated here. It is, however, possible to use the RRKM fits to extract the low pressure limiting values for the third-order rate constants for reference and comparison purposes. This has been done, and the values are tabulated in Table 7. This shows clearly that despite being a smaller molecule than SF_6, H_2O is more efficient than SF_6 as a third body stabilization partner for $H_2Si\cdots OH_2$* by a factor of between 2.5 and 4.3 depending on temperature and water isotopic species. This factor corresponds to the ratio k_3/k_2 in the mechanistic model. Despite some uncertainty (probably ca. ± 20%), this is a significant margin since SF_6 itself is estimated, from the RRKM calculations and the collisional model, to be ca. 89−96% efficient (β_c values) compared to the strong collision model.[31] This clearly points to an exceptional cross section or special interaction between the zwitterionic complex and the second water molecule.

Ab Initio Calculations and the Mechanism. The intermediate species and transition states for the SiH_4O surface were reported and discussed in detail earlier.[19] Those for the SiH_6O_2 surface are derived here for the first time. The results show that all the SiH_4O species identified earlier, including the transition states, can form effective hydrogen-bonded species with H_2O, in some cases in more than one form. These species are all stabilized by the hydrogen-bonding interaction with water. The extent of this stabilization is most marked for the zwitterion and its rearrangement activated complex, TS1. A comparison between the potential energy surfaces for SiH_4O and SiH_6O_2

for the key steps in the reaction of $SiH_2 + H_2O$ is shown in Figure 6. The crucial difference between the PE surfaces is that on SiH_4O, TS1 has a positive barrier of 26 kJ mol^{-1}, whereas on SiH_6O_2, TS1 has a negative barrier of 59 kJ mol^{-1}. The consequences of this are that without the assistance of a further H_2O molecule the zwitterionic complex $H_2Si\cdots OH_2$ is effectively the end product of the reaction of SiH_2 with H_2O, whereas with it the reaction system has a barrierless rearrangement to silanol $+ H_2O$. It is true that $H_2Si\cdots(OH_2)_2$ exists in a well of 44 kJ mol^{-1}, but since the hydrated zwitterion is formed from the hot $H_2Si\cdots OH_2^* + H_2O$, it should have enough internal energy to surmount this barrier without difficulty. Thus, the additional H_2O molecule is the effective catalyst for reaction, acting in the classic manner "by lowering the activation barrier".

This gas-phase catalytic effect provides the bridge which reconciles the gaseous and solution chemistry of reactions of silylenes with O-donors. The work of Weber's group showed that zwitterions were important as intermediates in solution studies. Our earlier work[19] and that of Alexander et al.,[20] backed by the theoretical calculations of Heaven et al.,[21] suggested that the gas-phase reaction of $SiH_2 + H_2O$ stopped at the zwitterion stage. Other studies of $SiH_2 + $ O-donors have shown the reversibility of zwitterion formation,[22] as did our own earlier work on $SiMe_2 + Me_2O$ and THF.[32] It is now clear that in both the gas phase and solution additional molecules of reactant (or solvent) are necessary to drive the reactions beyond the zwitterion stage.

There are parallels to our findings in other analogous systems. In the solution reactions of silenes with hydroxylated species,

ROH, Leigh's group[33−38] have observed kinetics that are in some cases second-order in [ROH]. The conclusions are similar, that nucleophilic ROH can assist (i.e., catalyze) the addition process, although in these reactions there is usually a competition between intramolecular and intermolecular mechanisms of product formation from the silene$\cdots$ROH complex. In another reaction system, Kudo and Gordon[39] have shown, via theoretical calculations, the involvement of multiple water molecules in the hydrolysis reactions of trichlorosilanes, in transition-state structures which have similarities with that of TS1 in Figure 4.

(32) Baggott, J. A.; Blitz, M. A.; Frey, H. M.; Lightfoot, P. D.; Walsh, R. *Int. J. Chem. Kinet.* **1992**, *24*, 127.

(33) Sluggett, G. W.; Leigh, W. J. *J. Am. Chem. Soc.* **1992**, *114*, 1195.
(34) Leigh, W. J.; Bradaric, C. J.; Kerst, C.; Banisch, J. A. *Organometallics* **1996**, *15*, 2246.
(35) Leigh, W. J.; Bradaric, C. J.; Sluggett, G. W.; Venneri, P. C.; Conlin, R. T.; Dhurjati, M. S. K.; Ezhova, M. B. *J. Organomet. Chem.* **1998**, *561*, 19.
(36) Morkin, T. L.; Leigh, W. J. *Acc. Chem. Res.* **2001**, *34*, 129 and references cited therein.
(37) Morkin, T. L.; Owens, T. R.; Leigh, W. J. Kinetics and Mechanisms of the Reactions of Si=C and Si=Si Double Bonds. In *The Chemistry of Organic Silicon Compounds*; Rappoport, Z., Apeloig, Y., Eds.; Wiley: Chichester, U.K., 2001; Vol. 3, Chapter 17, p 949 and references cited therein.
(38) Owens, T. R.; Harrington, C. R.; Pace, T. C.; Leigh, W. J. *Organometallics* **2003**, *22*, 5518.
(39) Kudo, T.; Gordon, M. S. *J. Phys. Chem. A* **2002**, *106*, 11347 and references cited therein.